J Mater Sci (2011) 46:992–998
DOI 10.1007/s10853-010-4857-x

Synthesis and characterization of Rosebengal/folicacid-functionalized multiwall carbon nanotubes

R. Anbarasan · C. A. Peng

Received: 2 July 2010 / Accepted: 19 August 2010 / Published online: 3 September 2010

Abstract Multiwall carbon nanotubes (MWCNTs) were functionalized with a photosensitizer, rosebengal (RB), and folicacid (FA), an anti-cancer drug simultaneously and individually, which was characterized with various analytical instruments like Fourier Transform Iinfrared (FTIR) spectroscopy, UV–Vis spectroscopy, Thermogravimetric analysis (TGA), Photoluminescence (PL) spectroscopy, X-ray photoelectron spectroscopy (XPS), and Transmission electron microscopy (TEM). FTIR spectra confirmed the chemical modification of MWCNT. The chemical functionalization of MWCNT with RB was further supported by UV–Vis and PL spectra.

Abbreviations

MWCNT	Multiwall carbon nanotube
FTIR	Fourier transform infrared
TGA	Thermogravimetric analysis
XPS	X-ray photoelectron spectroscopy
PLS	Photoluminescence spectroscopy
TEM	Transmission electron microscopy
NIR	Near infrared
PDT	Photodynamic therapy
RB	Rosebengal
FA	Folicacid
DI water	De-ionized water
DMF	Dimethylformamide

R. Anbarasan (✉)
Department of Mechanical Engineering, National Taiwan University, Taipei 10617, Taiwan, ROC
e-mail: anbu_may3@yahoo.co.in

C. A. Peng
Department of Chemical Engineering, National Taiwan University, Taipei 10617, Taiwan, ROC

Introduction

Carbon nanotubes (CNTs) on irradiation with Near Infrared (NIR) light have an ability for converting light into heat [1], which leads to a new branch in medicinal field called photodynamic therapy (PDT) with high performance, efficacy, and an economic way of treatment without any toxicity. The photochemical sensitizer on photochemical excitation generates singlet oxygen, which induces tumor destruction [2]. The combination of these two principles plays a vital role in cancer treatment. Bakalova et al. [3] revealed the requirements for an effective PDT. Moreover, they added that the photo sensitizer should be non-toxic, regioselective target of cancer cells, perform effective energy transfer to oxygen, be easily cleared from body, be resistant to aggregation, and be photo stable. Rosebengal (RB) [4, 5] is having such a qualification, and the singlet oxygen production by peptide-coated quantum dot photo sensitizer conjugates was reported by Tsay and co-workers [6]. Moczek et al. [7] investigated the singlet oxygen generation of RB-grafted chitosan. The insufficient lipophilicity and tumor accumulation of RB is rectified by conjugation with DMFC liposomes [8]. RB cross linked with cytoplasmic proteins is used in the live cells by multiphoton-excited microfabrication [9]. Binding of RB to serum albumin was reported in the literature [10]. White light-illuminated RB-coated cellulose acetate is used to kill the microbes [11].

Applications of CNTs are restricted to some extent because of its non-soluble nature. Such an insolubility problem can be outwitted by functionalization process [12]. In 2008, the properties and application as support for fuel cell of functionalized CNTs were reported by Rocco et al. [13]. MWCNTs are functionalized with cetyltrimethylammonium bromide [14], furfuryl alcohol [15], amidoamines [16],

polyimide [17], aniline [18], polymeric amines [19], octenyltrichlorosilane [20], aryl mercapto magnesium bromide [21], and poly(acrylic acid) [22]. In 2005, Hirsch et al. [23] reviewed the functionalization of CNTs.

Folic acid (FA) is an attractive target ligand due to its high binding affinity for the folate receptors ($K_d \sim 10^{-10}$ M). FA is efficiently internalized into the cells through the receptor-mediated endocytosis even when conjugated with a wide variety of molecules [24, 25]. FA and its conjugates were widely used for selective delivery of anticancer agents to cells with folate receptor, which were over-expressed in many kinds of human cancer cells such as ovarian, breast, and prostate cancers while only minimally distributed in normal tissues [26, 27]. Even after a thorough literature survey, we could not find any report based on photo sensitizer and cancer therapy simultaneously functionalized the MWCNT. In this communication, for the first time, we are reporting here about the characterizations of FA- and RB-functionalized MWCNT. These materials are having applications in the field of PDT to kill cancer cells.

Experimental

Materials

The MWCNT was received from CNT Company Limited, Taiwan and used as received. NaOH, HNO_3, and H_2SO_4 were obtained from Showa chemicals Limited, Japan. Sb_2O_3 and $SOCl_2$ were received from Seedchem Company Private Limited, Taiwan. Rose Bengal (RB) and FA were purchased from Sigma-Aldrich, USA. Dimethyl formamide (DMF, Across Organics, USA) was received and used without further purifications.

Functionalization of MWCNT by RB and FA

20 mg of MWCNT was dispersed in 10 mL of HNO_3/H_2SO_4 (1:3 volume ratio) at 80 °C for 24 h under stirring condition. After careful edge oxidation process, the products were filtered, washed five times with de-ionized (DI) water, and dried using vacuum freezer at 50 °C for 24 h. After drying, the samples were collected, weighed, and stored in a vial. The carboxyl edge-functionalized MWCNT thus obtained was dispersed in 15 mL of DMF under ultrasonic irradiation, and 5 mL of $SOCl_2$ was added slowly under stirring condition at room temperature. After the complete addition, the temperature was increased to 85 °C and maintained overnight under nitrogen atmosphere. The products were filtered, washed with DI water, and dried in vacuum freezer. The dried product was chlorinated MWCNT, and collected, weighed, and stored in a vial. Then, the obtained chlorinated MWCNT was dispersed in 15 mL of DI water under ultrasonication and 20 mg of RB or FA or RB + FA mixture was charged in a two-necked round-bottom flask, and stirred at 85 °C for 24 h. 0.03 g of Sb_2O_3, a condensation catalyst, was added, and the reaction was continued. NaCl was formed as a by-product, which can be removed from the reaction medium by repeated washing with excess of DI water. The product was washed and filtered until the filtrate became colorless. The filtrate from each washing was collected and subjected to UV–Vis spectral measurement by taking 2 mL of the sample quantitatively. The λ_{max} value was determined and detected from the λ_{max} value of pristine pure RB. The difference between λ_{max} values yielded the amount of RB chemically attached with the MWCNT, as 89.3%. In the investigation under this study, we used the 1:1 ratio of MWCNT and dye molecules. The product was dried under vacuum freezer for 24 h at room temperature. The samples were collected, weighed, and stored in a vial. The reaction is described in Scheme 1.

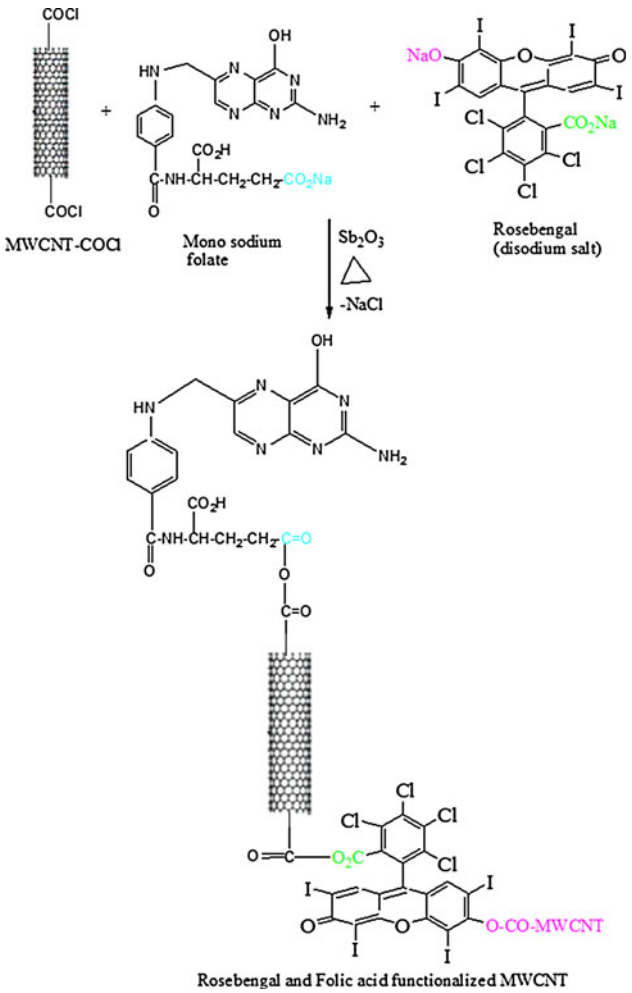

Scheme 1 Synthesis of RB/FA functionalized MWCNT

The black product obtained was the RB-, FA-, or RB + FA-functionalized MWCNT. The monosodium salt of FA was synthesized by titrating 0.50 N 20 mL of NaOH against the FA solution. The RB-functionalized MWCNT was soluble only after long time ultrasonic irradiation. The RB + FA- or FA-functionalized MWCNT was also soluble in water under short-time ultrasonic irradiation.

Characterizations

Before the analytical characterizations, the functionalized MWCNTs were repeatedly washed with DI water until the filtrate yielded a colorless solution. In such a way, the purity of the sample was confirmed as 100%. FTIR spectra for the samples were recorded with the help of Perkin Elmer Spectrum 100 series instrument by KBr pelletization method. Jasco V-570 instrument was used for UV–Vis spectrum measurements. Binding energy and % elements were determined from XPS Thermo Scientific-Theta Probe-Al radiation. XPS yielded more quantitative and useful information, and hence no need of elemental analysis. The thermal stability of the samples was analyzed using Rigagu TGA 8120 instrument under air purging at the heating rate of 10 °C min^{-1}. Jasco FP-6300 instrument was used for the PL measurement in an aqueous medium. Scheme 1 explains the binding of RB with MWCNT. The shorter wavelength UV-lamp was purchased from Spectroline UV-lamp, Japan. TEM was recorded with the help of TEM 3010, JEOL, and Japan instrument.

Results and discussion

FTIR study

Figure 1a shows the FTIR spectrum of pristine MWCNT. It shows one broad peak around 3443 cm^{-1} due to the OH-stretching vibration. Trace amounts of water molecules are attached with the MWCNT during the synthesis itself. Further, it can be confirmed by a peak at 1640 cm^{-1} occurring due to the bending vibration of water molecules. A broad peak at 592 cm^{-1} confirms the M–O (metal-oxide) stretching vibration (metal oxides used for the synthesis of MWCNT). Figure 1b indicates the FTIR spectrum of MWCNT-CO-RB conjugate. A broad peak at 3443 cm^{-1} describes the OH stretching of carboxyl group of unreacted OMWCNT. The C–H symmetric (2863 cm^{-1}) and anti-symmetric (2924 cm^{-1}) stretching are also seen. The carboxyl carbonyl stretching appears at 1640 cm^{-1}. Appearance of a broad peak at 1070 cm^{-1} explains the ester C–O–C linkage in the conjugate. The iodine (attached with RB) peak appears at 734 cm^{-1}. The appearance of new peaks due to I and C–O–C ester linkage confirms the binding of RB with MWCNT through diester linkage. Figure 1c,d indicates the FTIR spectrum of MWCNT functionalized with FA and RB + FA mixture, respectively. The new peaks that appear, particularly, the peaks at 1605 and 1326 cm^{-1} are corresponding to the amide C=O linkage and C–N stretching of FA-functionalized MWCNT. Peaks corresponding to halogen are appearing around 570 cm^{-1}. This observation confirms the chemical modification of MWCNT with RB + FA mixture. For the sake of comparison, the FTIR spectrum of pristine RB is also indicated in Fig. 1 as Fig. 1e. A broad peak at 3393 cm^{-1} is due to the OH stretching of water molecules associated with RB. The carbonyl stretching appears at 1620 cm^{-1}. The aromatic C–H stretching appears at 958 cm^{-1}. Peaks at 662 and 530 cm^{-1} are corresponding to Cl and I stretching vibrations.

UV–Vis spectroscopy

Absorbance spectrum of pristine RB is shown in Fig. 2a. A sharp peak at 558.9 nm confirmed the monomeric form of pristine RB. A small hump at 521.5 nm inferred the dimeric nature of RB. The absorbance spectrum of RB-conjugated MWCNT is shown in Fig. 2b. Here, one can observe the same pattern of peaks but with slight red shifting. The monomeric form of RB is seen at 565.9 nm, whereas the dimeric form is red shifted to 528.5 nm. During the functionalization reaction, RB can interact with MWCNT through alkoxide or ester linkage. The red shifting of monomeric as well as dimeric forms of RB confirmed the chemical binding of RB with MWCNT. Due to the formation of diester linkage, the absorption peak of RB was shifted to higher wavelength. In the present investigation, due to red shifting of absorption peak of RB,

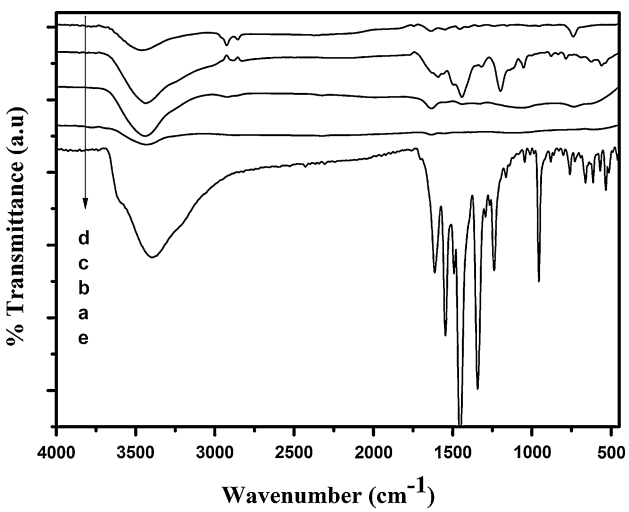

Fig. 1 FTIR spectra of (*a*) MWCNT, (*b*) MWCNT–RB, (*c*) MWCNT–FA, (*d*) RB–MWCNT–FA, (*e*) RB

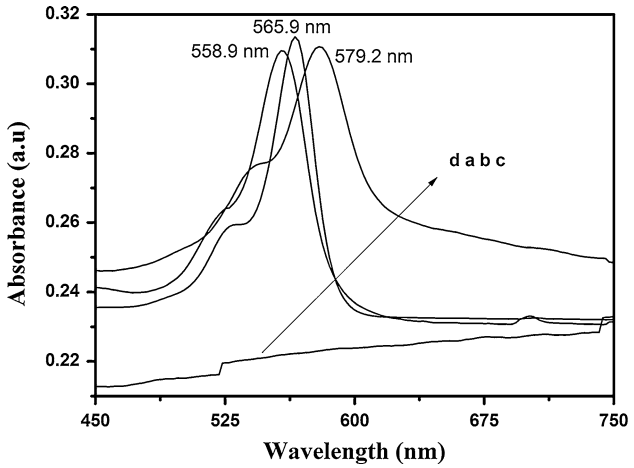

Fig. 2 UV–Vis spectrum of (*a*) pristine RB, (*b*) MWCNT–RB, (*c*) RB–MWCNT–FA, (*d*) FA

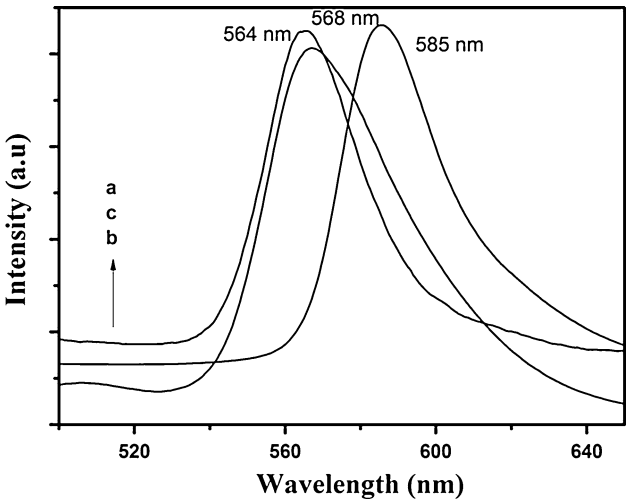

Fig. 3 PL spectrum of (*a*) pristine RB, (*b*) MWCNT–RB, (*c*) RB–MWCNT–FA

we can conclude that the binding takes place between RB and MWCNT preferably through diester linkage formation with slight alkoxide formation. Figure 2c exhibits the electronic absorption spectrum of simultaneous binding of RB (disodium salt) and FA (monosodium salt) with MWCNT. The monomeric and dimeric forms of RB were observed at 579.2 and 541.3 nm, respectively. In this case, due to the competitive bindings of RB and FA with MWCNT, the peak was red shifted. (For the sake of comparison, the UV–Vis spectrum of MWCNT–FA is given in Fig. 2d. No peak appeared around 560 nm). Appearance of these two peaks confirmed the simultaneous chemical binding of both RB and FA with MWCNT preferably through their ester linkage. Red shifting of complex made by RB with serum albumin was reported in the literature [24].

Photoluminescence study

Figure 3a indicates the PL spectrum of pristine RB with an emission peak at 564 nm. MWCNT after functionalization with RB (Fig. 3b) is showing a small hump at 568 nm. Figure 3c confirms the emission spectrum of MWCNT after functionalization with the mixture of FA and RB. Here, one can observe a broad peak at 585 nm. This red shift confirmed the role of FA on the functionalization with MWCNT in the presence of RB. Figure 4 indicates the photograph of MWCNT after functionalization with RB and FA. The pristine RB yielded a bright yellowish colour (Fig. 4a), whereas the RB- and RB + FA functionalized MWCNTs (Fig. 4b and c, respectively) showed the pale bluish colour. The MWCNT–FA (Fig. 4d) system too exhibited the pale bluish colour. The decrease in color intensity confirmed the chemical binding of MWCNT with

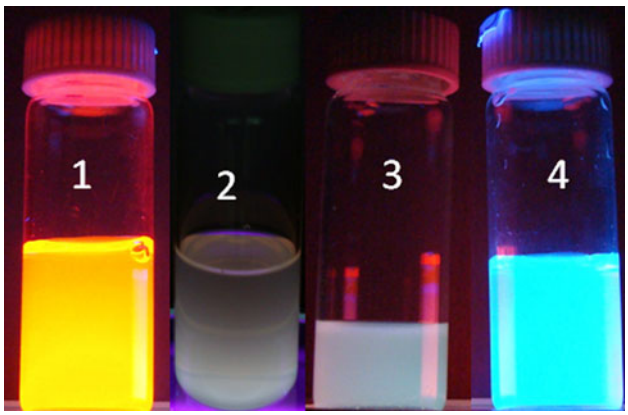

Fig. 4 Photograph taken under UV-irradiation of (*1*) RB, (*2*) MWCNT–RB, (*3*) FA–MWCNT–RB, (*4*) MWCNT–FA

FA and RB. The decrease in color intensity can be explained on the basis of quenching effect of MWCNT.

TGA history

The thermal stability of MWCNT before and after functionalization can be analyzed through TGA method. Figure 5a indicates the TGA of raw MWCNT. Up to 500 °C, weight loss due to degradation reaction of MWCNT was not observed. This confirmed the very high thermal stability of MWCNT. The thermogram of RB-conjugated MWCNT is represented in Fig. 5b. Up to 50 °C, it showed 4% weight loss due to the removal of moisture and, thereafter, no more weight loss was observed with the increase in temperature. This strongly supports the synthesis of thermally stable MWCNT-CO-RB. Figure 5c reveals the TGA thermogram of FA-functionalized MWCNT. Due to the presence of intermolecular hydrogen

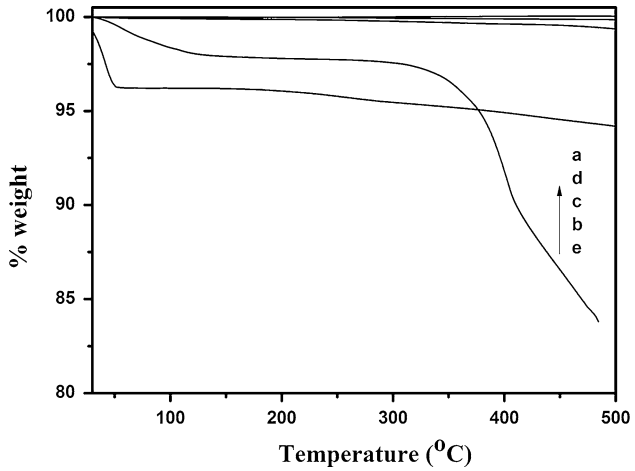

Fig. 5 TGA of (*a*) MWCNT, (*b*) MWCNT–RB, (*c*) MWCNT–FA, (*d*) FA–MWCNT–RB, (*e*) RB

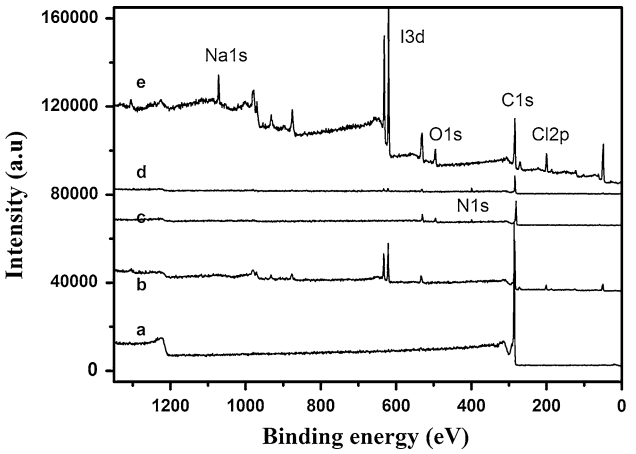

Fig. 6 XPS spectrum of (*a*) MWCNT, (*b*) MWCNT–RB, (*c*) MWCNT–FA, (*d*) FA–MWCNT–RB, (*e*) RB

bonding, the system showed higher thermal stability. Figure 5d represents the thermogram of FA + RB-functionalized MWCNT. The system in this study too exhibited the higher thermal stability owing to the presence of intermolecular forces. For the sake of comparison, the TGA of pristine RB is given in Fig. 5e. Pristine RB showed the multi-step degradation processes associated with the removal of water molecules, degradation of COONa, and degradation of ether linkage in RB. When comparing the thermal stability of MWCNT-CO-RB conjugate with that of pristine RB, the latter one showed less thermal stability. At 450 °C, the pristine RB showed 14% weight loss. Recently, Shih et al. [28] explained the thermal stability of functionalized MWCNT. Saeed and co-workers [29] discussed the thermal stability of amine-functionalized MWCNT, and the same showed the lower thermal stability than that of the pristine MWCNT.

XPS analysis

Figure 6a indicates the XPS spectrum of MWCNT. It shows the C1s peak at 283.3 eV. The XPS of MWCNT-CO-RB conjugate is shown in Fig. 6b. It shows C1s, O1s, Cl2p, and I3d peaks at 283.3, 533.2, 197.26, and 633.9 eV, respectively. The important point here is that a peak corresponding to Na1s at 1071 eV has completely disappeared. This confirms the existence of chemical binding between MWCNT and RB. During the conjugation reaction, the 2 moles of NaCl were eliminated as a by-product. Figure 6c indicates the XPS of FA-functionalized MWCNT. The N1s peak appears at 397.88 eV at the same time when the Na1s peak has disappeared. This confirms the chemical binding of FA with MWCNT. Figure 6d represents the XPS spectrum of MWCNT functionalized with RB + FA mixture (1:1 ratio) simultaneously. Peaks due to N1s, Cl2p, and I3d are appear with the disappearance of Na1s peak. This evidences the chemical interactions of both RB and FA with MWCNT. In both cases, the %N was found to be 1.65% (MWCNT–FA) and 0.33% (RB–MWCNT–FA), respectively. For the sake of comparison, the XPS of pristine RB is given in Fig. 6e. The Cl2p, C1s, O1s, I3d, and Na1s peaks were observed at 200.09, 283.95, 530.83, 619.86, and 1071.36 eV, respectively. The XPS confirms the structure of RB-bound MWCNT. Yong et al. [30] reported about the XPS of functionalized MWCNT. The binding energy of C1s of MWCNT was observed at 284.6 eV, and the O1s of oxidized MWCNT was seen at 532.3 eV [31]. Our investigations are in accordance with these two references [30, 31].

Table 1 provides the % elements of MWCNT before and after functionalization process. The raw MWCNT showed 99.9% C. On binding with RB, the %C was decreased to 92 whereas the % Cl was reduced to 1.56. This confirmed the removal of Cl^- ion from MWCNT as NaCl during the conjugation reaction of MWCNT with RB. The $\%I_2$ was found to be 3.58%. This is due to the attachment of RB with the chlorinated MWCNT. The pristine RB showed 53.61% C with 5.32% Na. After conjugation with MWCNT, the %C was raised with the disappearance of %Na. The reduction in %Cl after conjugation with MWCNT accounted for the

Table 1 XPS data

System	C (%)	O (%)	Cl (%)	I (%)	Na (%)	N (%)
MWCNT	99.99					
MWCNT–RB	85.92	08.94	1.56	03.58		
MWCNT–FA	80.15	18.20				1.65
RB–MWCNT–FA	84.57	12.63	0.99	1.48		0.33
RB	53.61	21.33	9.61	10.15	5.32	

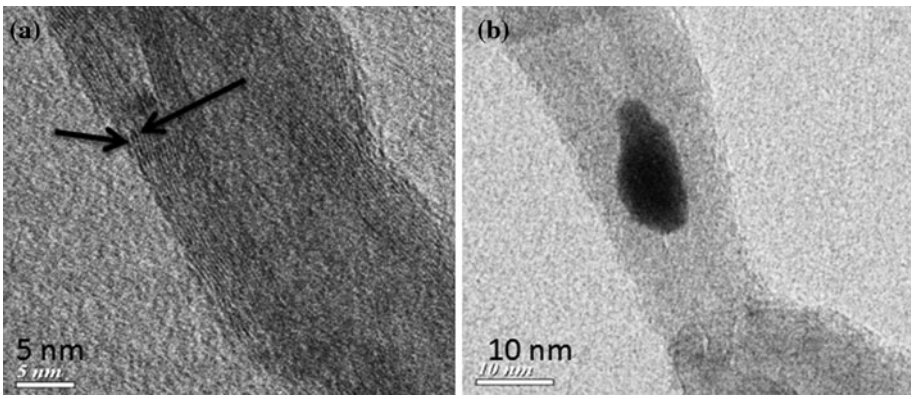

Fig. 7 TEM image of FA–MWCNT–RB

binding of RB to MWCNT with the simultaneous removal of NaCl, as a by-product.

TEM topography

Figure 7 exhibits the TEM images of RB + FA-functionalized MWCNT with layer-like structure (Fig. 7a). Figure 7b shows the functionalized MWCNT through the intercalation mechanism. This confirms the chemical binding of FA + RB with MWCNT.

Conclusions

In conclusion, we have successfully demonstrated the methodology for the functionalization of MWCNT with RB, a photo sensitizer, and with FA, a cancer therapy. The conjugate showed the absorption peak of monomeric form of RB at 558 nm which was greater than the absorption value of pristine RB. The MWCNT-conjugated RB did not show a peak corresponding to the Na1s in the XPS, and this confirmed the chemical conjugation of RB with MWCNT. Due to the presence of intermolecular forces, the FA- and FA + RB-functionalized MWCNT showed a higher thermal stability. The mixture of RB- and FA-functionalized MWCNT showed an emission peak at 585 nm. TEM confirmed the chemical modification of MWCNT with FA + RB mixture through the intercalation mechanism (i.e.,) formation of diester linkage.

Acknowledgement Dr.R.Anbarasan expresses his sincere thanks to the NTU, Taiwan and the NSC for their financial support during his postdoctoral research study at NTU, Taiwan.

References

1. Pavitra C, Marches R, Zimmerman NS, Vitetta ES (2008) PNAS 105:8697. doi:10.1073/pnas.0803557105
2. Ishibashi T, Lee CI, Okabe E (1996) J Pharmacol Exp Therapy 277:350
3. Bakalova R, Ohba H, Baba Y (2004) Nano Lett 4:1567. doi:10.1021/nl049627w
4. Lampert CR, Kochevar IE (1996) J Am Chem Soc 118:3297. doi:10.1021/ja9600800
5. Singh RJ, Hogg N, Kalyanaraman B (1995) Arch Biochem Biophys 324:367
6. Tsay JM, Trzoss M, Shi L, Weiss S (2007) J Am Chem Soc 129:6865. doi:10.1021/ja0707131o
7. Moczek L, Nowakowska M (2007) Biomacromolecules 8:433. doi:10.1021/bm060454t
8. Chang CC, Yang YT, Yang JC, Tsai T (2008) Dyes Pigment 79:170. doi:10.1016/j.dyepig.2008.02.003
9. Swarna B, Rodinov V, Teresaki M (2005) Opt Lett 30:159. doi:10.1364/0l.30.00019
10. Abuin E, Aspee A, Lishi E, Leon L (2007) J Chil Chem Soc 52:1196. doi:10.4067/s0717-97-072007000200017
11. Decrene V, Pratten J, Wilson M (2006) Appl Environ Microbiol 72:4436. doi:10.1128/AEM.02915-05
12. Peng Q, Qu L, Dai L, Vaia RA (2008) ACS Nano 2:1833. doi:10.1021/nn8002532
13. Rocco AM, Macedo MIF, Maestro LF, Herbst MH, Xavier AL (2008) J Mater Sci 43:557. doi:10.1007/s10853-007-1779-3
14. Li Q, Xue Q, Hao L, Gao X, Zheng Q (2008) Compos Sci Tech 68:2290. doi:10.1016/j.compscitech.2008.04.019
15. Men XH, Zhang ZZ, Song HJ, Wang K (2008) Compos Sci Tech 68:1042. doi:10.1016/j.compscitech.2007.07.008
16. Lin ST, Wei KL, Lee TM, Lin JJ (2006) Nanotechnology 17:3197. doi:10.1088/0957-4484/17/13/020
17. Singh BP, Singh D, Mathur RB (2008) Nano Scale Res Lett 3:444. doi:10.1007/s11671-008-9179-4
18. Karousis N, Boucetta HA, Tegmatarchis N (2008) Mater Sci Eng B 152:8. doi:10.1016/j.mseb.2008.06.002
19. Zhang Y, Stuart MCA, Picchioni F (2008) Macromolecules 41:6141. doi:10.1021/ma800869w
20. Vast L, Carpentier L, Lallemand F, Colomer J-F, Van Tendeloo G, Fonseca A, Nagy JB, Mekhalif Z, Delhalle J (2009) J Mater Sci 44:3476. doi:10.1007/s10853-009-3464-1
21. Xu G, Wu WT, Wang Y, You Y (2006) Polymer 47:5909. doi:10.1016/j.polymer.2006.06.027
22. Guo G, Qin F, Yang D, Yang S (2008) Chem Mater 20:2291. doi:10.1021/cm703225p
23. Hirsch A, Vostrowsky O (2005) Top Curr Chem 245:193. doi:10.1007/b98169
24. Biswas S, Bhattarcharjee D, Hussain SA (2007) J Colloid Inter Sci 311:361. doi:10.1016/j.jcis.2007.03.055
25. Turek JJ, Leamon CP, Low PS (1993) J Cell Sci 106:423

26. Dixit V, Van den Bossche J, Sherman DM, Thompson DH, Andres RP (2006) Bioconjugate Chem 17:603. doi:10.1021/bc050335b
27. Pan D, Turner JL, Wooley KL (2003) Chem Commun 19:2400. doi:10.1039/b307878g
28. Shih YF, Chen LS, Jeng RJ (2008) Polymer 49:4602. doi:10.1016/j.polymer.2008.08.015
29. Saeed K, Park SY, Lee HJ, Huh WS (2006) Polymer 47:8019. doi:10.1016/j.polymer.2006.09.012
30. Yong XG, Ru X, Hu W, Ren ZQ (2008) Chin Sci Bull 53:2297. doi:10.1007/s11434-008-0317-2
31. Xu G, Wu WT, Wanf P, Lu F (2006) Nanotechnology 17:2458. doi:10.1088/0957-4484/17/10/005